

Oxidative C–H Homocoupling of Push–Pull Benzothiazoles: An Atom-Economical Route to Highly Emissive Quadrupolar Arylamine-Functionalized 2,2'-Bibenzothiazoles with Enhanced Two-Photon Absorption

Patrik Osuský, Jela Nociarová, Maroš Smolíček, Róbert Gyepes, Dimitris Georgiou, Ioannis Polyzos, Mihalis Fakis, and Peter Hrobárik*

Cite This: *Org. Lett.* 2021, 23, 5512–5517

Read Online

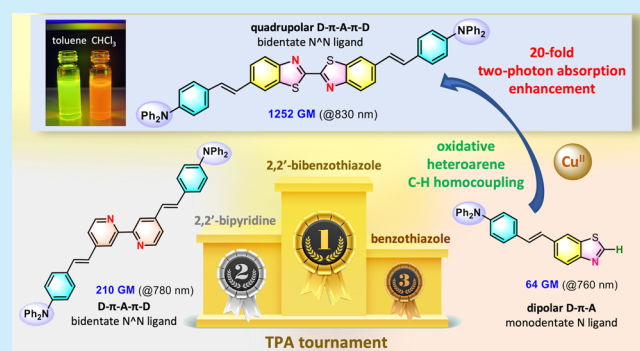
ACCESS |

Metrics & More

Article Recommendations

Supporting Information

ABSTRACT: Copper(II)-catalyzed C–H/C–H coupling of dipolar 2-*H*-benzothiazoles end-capped with triphenylamine moieties affords highly fluorescent 2,2'-bibenzothiazoles with quadrupolar (D- π -A- π -D) architecture displaying large two-photon absorption (TPA) cross sections (543–1252 GM) in the near-infrared region. The notably higher TPA performance as compared to quadrupolar π -systems with a widely used 2,2'-bipyridine core, along with the ease of the synthesis and chelating N^N ability, makes the title biheteroaryl platform an attractive building block for a large scope of functional dyes exploiting nonlinear optical phenomena.



Nonlinear optical (NLO) media are among the smartest materials giving rise to modern laser technologies, including ultrafast all-optical signal processing,¹ high-capacity optical data storage,² or 3D microfabrication.³ NLO active molecules are also vital in high-resolution bioimaging, exploiting a second-harmonic generation⁴ and/or two-photon-excited fluorescence (TPEF),⁵ and they serve as singlet oxygen photosensitizers in photodynamic therapy (PDT)^{6,7} by using near-IR light. The latter two techniques take advantage of the two-photon absorption (TPA)—the third-order phenomenon referring to a simultaneous absorption of two photons of half the nominal excitation energy by a single molecule. This process enables the excitation of molecules by low-energy light in the biological transparency window (700–1000 nm), which is beneficial in an in-depth tissue/material penetration as compared to one-photon absorption (OPA) in the visible region and allows more control and higher spatial resolution via quadratic dependence of the TPA rate on the incident laser light intensity.^{5,6}

Applications of conventional OPA dyes in TPEF microscopy or two-photon-excited PDT suffer from small TPA cross sections, δ_{TPA} often limited to a few tens of GM units. These require high laser powers and long exposure times, which may result in photochemical damage of an irradiated object. To fully benefit from the advantages of TPA, a quest for dyes possessing large δ_{TPA} values, together with high quantum yields, good photostability, and cell permeability (keeping thus molecular

size as small as possible), is still a hot topic in material science.^{5,6,8}

In this regard, employment of suitable heteroaromatic scaffolds in π -conjugated systems with intramolecular charge-transfer (ICT) is a useful design strategy in the construction of TPA active dyes allowing researchers to meet specific application requirements and to achieve large δ_{TPA} values within a confined chromophore space by proper arrangement of heteroatoms or entire heteroaromatic blocks within the π -system.^{5–9} Of particular popularity are low-cost and readily available *N*-heteroaromatics, such as pyridines (py's), pyrazines (pz's), 2,2'-bipyridines (bpy's), or benzothiazoles (btz's), owing to their electron-accepting properties, photochemical resistance, and ease of their further functionalization through protonation, *N*-alkylation, or *N*-coordination to metal fragments allowing to tune solubility and NLO properties of π -systems thereof.^{7,9–14}

In most benzothiazole-derived π -conjugated systems reported so far, electron-donating triarylamine moieties are attached to the heteroarene C-2 position due to its higher reactivity, which however limits their further facile functionalization at the less

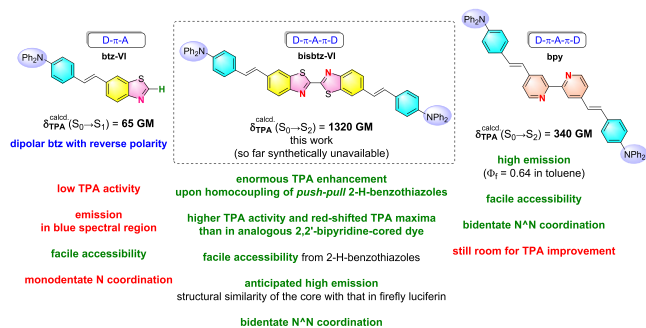
Received: June 4, 2021

Published: July 7, 2021



reactive benzene ring.¹² In addition, we have shown that placing triarylamine branches to the C-6 position of the **btz** unit is more favorable in terms of larger TPA activity, especially when the auxiliary electron-withdrawing group (EWG) is attached to the C-2 carbon.⁸ While dipolar C-6 substituted 2-*H*-benzothiazoles without an additional EWG substituent display small TPA action cross sections comparable with other commonly used OPA fluorophores,⁸ our latest DFT computational studies revealed that the TPA activity of these derivatives should be largely enhanced (>20-fold) by their transformation to hitherto elusive quadrupolar 2,2'-biphenylbenzothiazoles (Scheme 1). The

Scheme 1. DFT (CAM-B3LYP/6-311++G)¹⁵ Computed TPA Cross Sections, δ_{TPA} , in Their Low-Energy Resonant Maxima ($S_0 \rightarrow S_1$ for D- π -A, $S_0 \rightarrow S_2$ for D- π -A- π -D) for Pertinent Triphenylamine-Functionalized 2-*H*-Benzothiazole (left), 2,2'-Biphenylbenzothiazole (middle), and 2,2'-Bipyridine (right) Together with Their Advantageous/Disadvantageous Features^a**



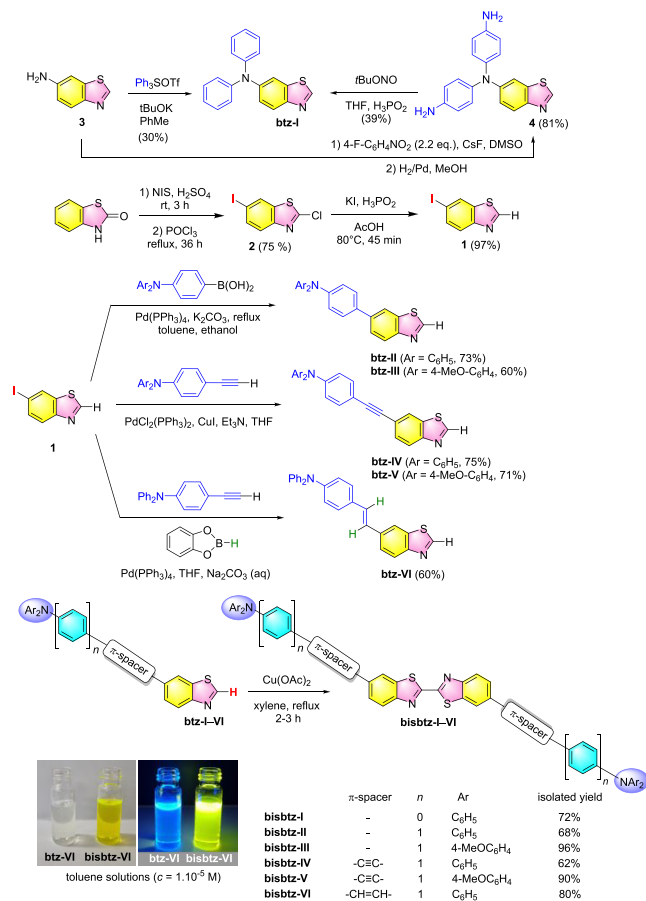
^aSee SI for computational details and analysis.

latter derivatives are also expected to show high emission quantum yields due to the structural similarity of their π -core with the skeleton of firefly luciferin, and they could benefit from feasible bidentate N*N coordination, resembling the chemistry of bipyridine-cored π -systems widely used in NLO applications,^{7,11–13} but with higher TPA efficiency.

Although unsubstituted 2,2'-biphenylbenzothiazole (bisbtz) has recently attracted the attention of material chemists as a bidentate N*N ligand in the construction of efficient red- or NIR-light emitters for OLED devices,¹⁶ its triarylamine-functionalized derivatives have remained so far synthetically unavailable and their properties unexplored.

To prove the anticipated TPA performance of this quadrupolar heteroaromatic platform, we first developed a facile access to a variety of dipolar (D- π -A) 2-*H*-benzothiazoles (**btz-I–VI**) bearing arylamine moieties attached to the C-6 position of the heteroaromatic scaffold via π -spacers of different length. A key intermediate, 6-iodobenzothiazole (**1**), was prepared by a quantitative hydrodechlorination of 6-iodo-2-chloro-benzothiazole (**2**) with KI and H₃PO₂. Compound **2** was obtained by direct iodination of commercially available 2-chlorobenzothiazole with I₂/KMnO₄ or in higher yield using a two-step sequence-selective C-6 iodination of benzothiazol-2(3*H*)-one and subsequent chlorination with POCl₃ (Scheme 2).^{10c} Triarylamine moieties with or without a π -spacer were introduced to the benzothiazole scaffold via Pd-catalyzed cross-coupling reactions of **1** with corresponding arylacetylenes, arylboronic acids, or in situ generated arylvinylboronic acids under Sonogashira and Suzuki-type conditions, respectively (Scheme 2). The derivative with the shortest π -conjugation, **btz-**

Scheme 2. Synthesis of Dipolar (D- π -A) Arylamine-Functionalized 2-*H*-Benzothiazoles and Their Transformation to Quadrupolar 2,2'-Biphenylbenzothiazoles by Cu^{II}-Mediated Oxidative Homocoupling^a



^aVisual demonstration of the changes in absorption and emission (under 365 nm UV light) of **btz** and **bisbtz** derivatives.

I, was obtained in a reasonable yield by direct arylation of readily available benzothiazole-6-amine (**3**) with a highly reactive triphenylsulfonium triflate (Ph₃SOTf).¹⁷ Attempts to introduce a NPh₂ group to **1** by means of Buchwald–Hartwig amination¹⁸ with diphenylamine were unsuccessful, while the coupling of **3** with bromobenzene afforded a mixture of *N*-monoarylated amine and *N*,2-diphenylbenzothiazole-6-amine (see SI). To avoid the undesired C-2 arylation, we also explored a route starting by aromatic nucleophilic substitution of **3** with 2.2 equiv of 4-fluoronitrobenzene, followed by reduction with H₂/Pd and hydrodeamination of the two pendant amino groups in **4** by *t*BuONO/THF and an aqueous solution of H₃PO₂, which afforded **btz-I** from **3** in the overall yield only slightly higher than that of the direct arylation.

The push–pull 2-*H*-benzothiazoles (**btz-I–VI**) were subsequently transformed to the desired 2,2'-biphenylbenzothiazoles in one-step oxidation reaction by inexpensive and commonly used Cu(OAc)₂,¹⁹ affording the products in 62–96% yields (Scheme 2).

This synthetic approach takes advantage of oxidative C–H homocoupling, which is a convenient and atom-economical method for the construction of bi(hetero)aryl skeletons.²⁰ While the homocoupling of donor-substituted 2-*H*-benzothiazoles in xylene proceeds also with the substoichiometric amount of

$\text{Cu}(\text{OAc})_2$, the reaction requires a much longer reaction time until complete conversion (ca. 36 h when using 0.2 equiv of oxidant). The reaction can be accelerated by using nitrobenzene as the solvent, but due to its toxicity and very high boiling point we find xylene to be a more convenient medium (see SI).

Structures of all **bisbtz** species were confirmed spectroscopically and by elemental analysis, while representative **bisbtz-I** was also characterized by single crystal X-ray diffraction (Figure 1),

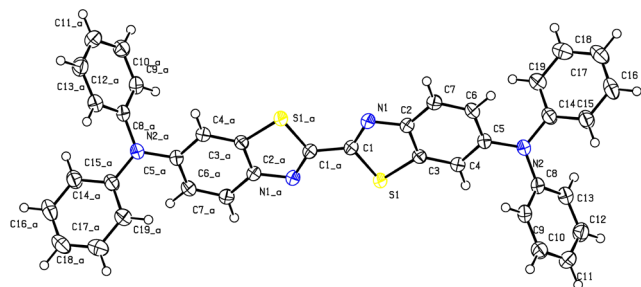


Figure 1. Molecular structure of **bisbtz-I**. Solvent molecules are omitted for clarity, and the displacement ellipsoids are drawn at the 50% probability level (see SI for more details).

showing a coplanar arrangement of two benzothiazole rings in the core. The C–C distance between two btz moieties is 1.456(2) Å, hinting at the efficient π -conjugation throughout the entire backbone with a partial $\text{C}_{\text{btz}}=\text{C}_{\text{btz}}$ double-bond character. In line with DFT calculations, two heteroarene moieties adopt the energetically favorable *s-trans* configuration, while *s-cis* conformers are computed to be thermodynamically less stable by ca. 24 kJ/mol.

Target **bisbtz** dyes were subjected to measurements of UV–vis absorption and emission spectra (Figures 2a,b), as well as to TPA cross sections, δ_{TPA} , via a TPEF method with femtosecond laser excitation at wavelengths of 730–870 nm (Figure 3). The squared dependence of up-converted fluorescence intensity on input laser power, confirming a two-photon excitation mechanism, is shown in Figure S10 in the SI. One-photon and two-photon spectral characteristics are summarized in Table 1.

The absorption spectra of **bisbtz** dyes in toluene (Figure 2a) feature an intense band in the visible region with maxima λ_{abs} positioned at 419–450 nm. According to time-dependent DFT calculations, the low-energy transitions are associated with an intramolecular charge-transfer (ICT) from electron-rich arylamines to the bisbtz core (see HOMO and LUMO orbitals in Figure 2d). Note that some **bisbtz** derivatives display a distinct shoulder peak on the low-energy side and this two-component pattern is also seen in the emission spectra, which can be related to the vibronic coupling. The fluorescence in toluene (Figures 2b,c) is observed in the green spectral region with the most intense peaks at 495–527 nm, reaching very high emission quantum yields Φ_f 's of 0.68–0.99. The fluorescence dynamics exhibits a biexponential decay with a fast component with a lifetime of 0.36–0.65 ns and a slower one of 1.42–2.46 ns (Figure 2e, Table S1 in SI). The slower component is considered as the main population decay mechanism while the faster one could be attributed to nonradiative decay due to conformational relaxation phenomena. The averaged lifetime (τ) values of derivatives bearing pendant methoxy groups (**bisbtz-III**, **bisbtz-V**) are longer than those of the other dyes, pointing to a stronger stabilization of their excited state due to the +M effect of OMe functionalities (Table 1).

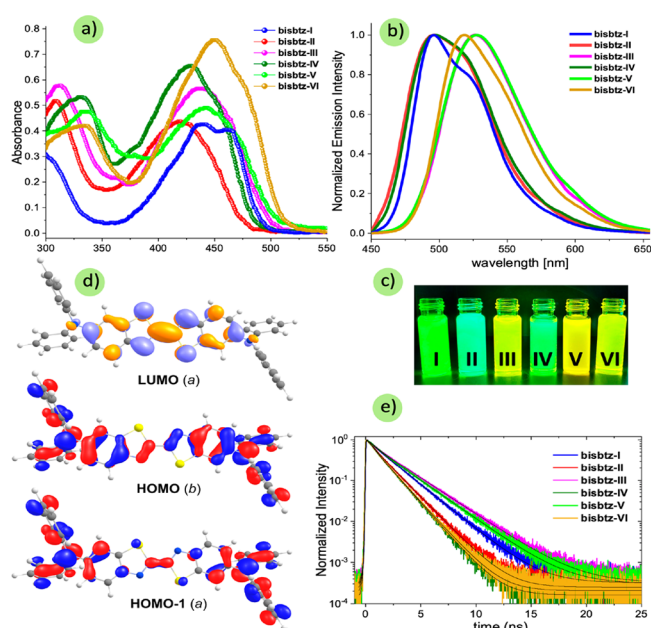


Figure 2. (a) UV–vis absorption ($c = 1 \times 10^{-5}$ M) and (b, c) emission ($c = 5 \times 10^{-6}$ M) of **bisbtz** dyes in toluene. (d) Frontier MOs of **bisbtz-I** relevant to intensive, lowest-energy OPA ($S_0 \rightarrow S_1$; HOMO \rightarrow LUMO) and TPA ($S_0 \rightarrow S_2$; HOMO – 1 \rightarrow LUMO) transitions. (e) Nanosecond fluorescence dynamics for the **bisbtz** dyes in toluene solution ($c = 5 \times 10^{-6}$ M). The excitation wavelength was 400 nm, and the detection was at the wavelength of emission maxima.

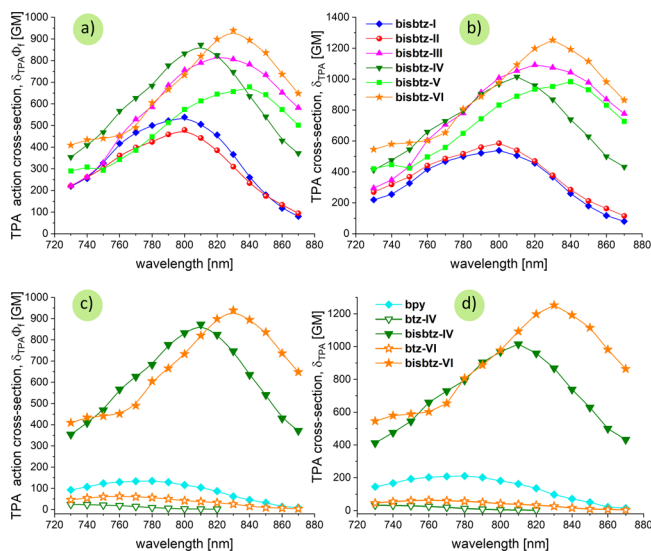


Figure 3. (a) TPA action cross sections, $\delta_{\text{TPA}}\Phi_f$ and (b) TPA cross sections, δ_{TPA} , of **bisbtz** dyes in toluene ($c = 2 \times 10^{-5}$ M). (c) Comparison of TPA action cross sections and (d) TPA cross sections of **bisbtz-IV** and **bisbtz-VI** with their dipolar congeners (**btz-IV**, **btz-VI**) and a bipyrindine-cored quadrupole **bpy**. TPEF referenced to Rhodamine 6G ($c = 2 \times 10^{-5}$ M) in methanol as the standard (see SI for more details).

Importantly, all **bisbtz** fluorophores exhibit high TPA cross sections, $\delta_{\text{TPA}} = 543$ –1252 GM, exceeding those of many one-photon fluorophores²¹ and parent dipolar 2-*H*-benzothiazoles **btz** by more than an order of magnitude (Figure 3d), confirming thus the efficiency of the synthetic strategy (homocoupling of arylamine-functionalized C–H heteroarenes) in large TPA enhancement. TPEF maxima positions λ_{TPA} (800–840 nm) are

Table 1. Photophysical Properties of 2,2'-Bibenzothiazoles bisbtz-I–VI in Comparison with Pertinent Dipolar 2-H-Benzothiazoles and bpy Congener of bisbtz-VI in Toluene

dye	λ_{abs} [nm]	ϵ_{abs} [M ⁻¹ cm ⁻¹]	λ_{f} [nm]	Φ_{f}	$\langle\tau\rangle$ [ns]	λ_{TPA} [nm]	$\delta_{\text{TPA}}\Phi_{\text{f}}$ [GM]	δ_{TPA} [GM]
bisbtz-I	439	42 500	495	0.99	1.70	800	538	543
bisbtz-II	419	43 700	496	0.82	1.34	800	480	585
bisbtz-III	437	55 600	527	0.75	2.00	820	819	1092
bisbtz-IV	428	65 100	497	0.86	1.22	810	873	1015
bisbtz-V	441	49 000	527	0.68	1.92	840	679	998
bisbtz-VI	450	74 300	518	0.75	1.24	830	939	1252
btz-IV	365	31 500	405	0.75		730	34	46
btz-VI	381	34 500	429	0.96		760	62	64
bpy	392	52 100	443	0.64		780	135	210

less than twice that of the single-photon absorption λ_{abs} ($S_0 \rightarrow S_1$), implying a deeper $S_0 \rightarrow S_2$ transition associated mainly with the HOMO – 1 \rightarrow LUMO excitation. Both of these MOs have the same *a* symmetry, obeying thus a parity selection rule for quadrupolar dyes (see also Figure S9 and Table S9 in SI).

TPA cross sections of resonant maxima increase within the bisbtz series nonmonotonically along with the elongation of the π -conjugation length, while the vinylene π -spacer is found to be more efficient than the ethynylene linkage. Interestingly, the introduction of peripheral methoxy groups to bisbtz-II led to an approximately 2-fold TPA enhancement, while the same modification in the longer π -system (bisbtz-IV \rightarrow bisbtz-V) affected TPA activity marginally.

It is noteworthy that the TPA maximum cross section of bisbtz-VI is ca. 6 times larger than that of bipyridine-cored congener bpy^{12,13} measured in toluene under identical TPEF conditions (literature data for bpy are 219 GM at 690 nm and 425 GM at 780 nm in chloroform and DMF, respectively).^{12,13} Although the TPA performance of bisbtz-VI in chloroform is somewhat lowered ($\delta_{\text{TPA}} = 1018$ GM at 840 nm), it is still about 4.6 times higher than that of bpy, yet with an emission maximum shifted to the orange spectral region (Figures S4 and S12 in SI). The TPA superiority of the bisbtz scaffold can be ascribed according to the three-state model²² to a notably larger transition-dipole moment between the ground and the first excited state ($\mu_{01} = 17.8$ D), which is also reflected in the higher molar extinction coefficient (cf. ϵ_{abs} for bisbtz-VI and bpy in Table 1), larger first-excited-to-second-excited state transition moment ($\mu_{12} = 13.4$ D), and smaller detuning energy ($E_1 - E_2/2 = 1.32$ eV) as compared to the bpy-cored congener with $\mu_{01} = 14.4$ D, $\mu_{12} = 9.9$ D, and $E_1 - E_2/2 = 1.65$ eV. This, in turn, allows researchers to achieve higher TPA activity within the confined chromophore space with a shorter π -bridge, that is beneficial in the engineering of small-molecular probes for TPEF microscopy or photosensitizers for PDT.

In addition, our pilot studies on the complexation of bisbtz-I with transition-metal carbonyl compounds, such as $\text{ReCl}(\text{CO})_5$, confirmed its bidentate N^{^N} coordination, while forming a purple complex $[\text{ReCl}(\text{CO})_3(\text{bisbtz-I})]$ with low-energy ICT absorption bands positioned at 536 and 562 nm (Figure S5 in SI). Complexation via central azole N^{^N} nitrogen atoms is unambiguously manifested by a high-frequency ¹⁵N NMR azole shift from –70 ppm in the free ligand (bisbtz-I) to –123 ppm in the Re^{I} complex, which is in excellent agreement with the ¹⁵N NMR shifts computed for the considered species by means of relativistic calculations (Table S11 in SI).²³

To conclude, homocoupling of push–pull C–H heteroarenes is demonstrated to be a simple and atom-economical strategy to achieve large (~20-fold) TPA enhancement. Outstanding one-

photon and two-photon absorption properties in the visible and near-IR region, respectively, along with the chelating N^{^N} ability, make triarylamine-functionalized 2,2'-bibenzothiazoles a more attractive alternative to notorious donor-functionalized 2,2'-bipyridines. On the basis of the high TPA cross sections, strong emission, and bidentate coordination, the title quadrupolar biheteroarenes provide a privileged platform paving the way to a large scope of efficient, small- to medium-sized, NLO-phores with diverse (dipolar, quadrupolar, octupolar) architectures, properties of which can be easily tailored by modifying the peripheral arylamine moieties and/or metal fragments.

■ ASSOCIATED CONTENT

SI Supporting Information

The Supporting Information is available free of charge at <https://pubs.acs.org/doi/10.1021/acs.orglett.1c01861>.

Experimental and computational details, synthetic procedures, compound characterization, crystal structure data for bisbtz-I, and computed TPA cross sections (PDF)

FAIR data, including the primary NMR FID files, for compounds 1–4, btz-I–VI, bisbtz-I–VI (ZIP)

■ Accession Codes

CCDC 2056840 contains the supplementary crystallographic data for this paper. These data can be obtained free of charge via www.ccdc.cam.ac.uk/data_request/cif, or by emailing data_request@ccdc.cam.ac.uk, or by contacting The Cambridge Crystallographic Data Centre, 12 Union Road, Cambridge CB2 1EZ, UK; fax: +44 1223 336033.

■ AUTHOR INFORMATION

Corresponding Author

Peter Hrobárik – Department of Inorganic Chemistry, Faculty of Natural Sciences, Comenius University, SK-84215 Bratislava, Slovakia; Laboratory for Advanced Materials, Comenius University Science Park, SK-84215 Bratislava, Slovakia; orcid.org/0000-0002-6444-8555; Email: peter.hrobarik@uniba.sk

Authors

Patrik Osuský – Department of Inorganic Chemistry, Faculty of Natural Sciences, Comenius University, SK-84215 Bratislava, Slovakia

Jela Nociarová – Department of Inorganic Chemistry, Faculty of Natural Sciences, Comenius University, SK-84215 Bratislava, Slovakia

Maroš Smolíček – Department of Inorganic Chemistry, Faculty of Natural Sciences, Comenius University, SK-84215 Bratislava, Slovakia

Róbert Gyepes – Faculty of Science, Charles University in Prague, CZ-12843 Prague, Czech Republic; orcid.org/0000-0002-2908-0425

Dimitris Georgiou – Department of Physics, University of Patras, GR-26504 Patras, Greece

Ioannis Polyzos – Department of Physics, University of Patras, GR-26504 Patras, Greece

Mihalis Fakis – Department of Physics, University of Patras, GR-26504 Patras, Greece; orcid.org/0000-0003-0801-7029

Complete contact information is available at:

<https://pubs.acs.org/10.1021/acs.orglett.1c01861>

Notes

The authors declare no competing financial interest.

ACKNOWLEDGMENTS

This work was supported by the Slovak Research and Development Agency (Grant No. APVV-17-0324), the Grant Agency of the Ministry of Education of the Slovak Republic (VEGA Project No. 1/0712/18), as well as by the European Union's Horizon 2020 research and innovation programme under Grant No. 810701 (LAMatCU) and the Marie Skłodowska-Curie Grant No. 752285.

REFERENCES

- (1) Barlow, S.; Bredas, J. L.; Getmanenko, Y. A.; Gieseck, R. L.; Hales, J. M.; Kim, H.; Marder, S. R.; Perry, J. W.; Risko, C.; Zhang, Y. Polymethine materials with solid-state third-order optical susceptibilities suitable for all-optical signal-processing applications. *Mater. Horiz.* **2014**, *1*, 577–581 and references cited therein.
- (2) Walker, E.; Rentzepis, P. M. Two-photon technology: a new dimension. *Nat. Photonics* **2008**, *2*, 406–408.
- (3) See, e.g.: (a) Kawata, S.; Sun, H. B.; Tanaka, T.; Takada, K. Finer features for functional microdevices. *Nature* **2001**, *412*, 697–698. (b) Zhou, W. H.; Kuebler, S. M.; Braun, K. L.; Yu, T. Y.; Cammack, J. K.; Ober, C. K.; Perry, J. W.; Marder, S. R. An efficient two-photon-generated photoacid applied to positive-tone 3D microfabrication. *Science* **2002**, *296*, 1106–1109. (c) Li, Z. Q.; Pucher, N.; Cicha, K.; Torgersen, J.; Ligon, S. C.; Ajami, A.; Husinsky, W.; Rosspointner, A.; Vauthey, E.; Naumov, S.; Scherzer, T.; Stampfl, J.; Liska, R. A straightforward synthesis and structure–activity relationship of highly efficient initiators for two-photon polymerization. *Macromolecules* **2013**, *46*, 352–361.
- (4) For a representative review, see, e.g.: Reeve, J. E.; Anderson, H. L.; Clays, K. Dyes for biological second harmonic generation imaging. *Phys. Chem. Chem. Phys.* **2010**, *12*, 13484–13498.
- (5) For TPEF reviews, see, e.g.: (a) Xu, L.; Lin, W.; Huang, B.; Zhang, J.; Long, X.; Zhang, W.; Zhang, Q. The design strategies and applications for organic multi-branched two-photon absorption chromophores with novel cores and branches: a recent review. *J. Mater. Chem. C* **2021**, *9*, 1520–1536. (b) Yao, S.; Belfield, K. D. Two-Photon Fluorescent Probes for Bioimaging. *Eur. J. Org. Chem.* **2012**, *2012*, 3199–3217. (c) Pawlicki, M.; Collins, H. A.; Denning, R. G.; Anderson, H. L. Two-photon absorption and the design of two-photon dyes. *Angew. Chem., Int. Ed.* **2009**, *48*, 3244–3266.
- (6) For PDT reviews, see, e.g.: (a) Xu, L.; Zhang, J.; Yin, L.; Long, X.; Zhang, W.; Zhang, Q. Recent progress in efficient organic two-photon dyes for fluorescence imaging and photodynamic therapy. *J. Mater. Chem. C* **2020**, *8*, 6342–6349. (b) Bolze, F.; Jenni, S.; Sour, A.; Heitz, V. Molecular photosensitisers for two-photon photodynamic therapy. *Chem. Commun.* **2017**, *53*, 12857–12877.
- (7) Karges, J.; Kuang, S.; Maschietto, F.; Blacque, O.; Ciofini, I.; Chao, H.; Gasser, G. Rationally designed ruthenium complexes for 1- and 2-photon photodynamic therapy. *Nat. Commun.* **2020**, *11*, 3262.
- (8) See, e.g.: (a) Durand, N.; Mhanna, R.; Savel, P.; Akdas-Kiliç, H.; Malval, J.-P.; Soppera, O.; Fillaut, J.-L. Unexpected disruption of the dimensionality-driven two-photon absorption enhancement within a multipolar polypyridyl ruthenium complex series. *Chem. Commun.* **2020**, *56*, 12801–12804. (b) Vakuliuk, O.; Jun, Y. W.; Vygranenko, K.; Clermont, G.; Reo, Y. J.; Blanchard-Desce, M.; Ahn, K. H.; Gryko, D. T. Modified Isoindole-1-one as Bright Fluorescent Probes for Cell and Tissue Imaging. *Chem. - Eur. J.* **2019**, *25*, 13354–13362. (c) Zhou, R.; Malval, J.-P.; Jin, M.; Spangenberg, A.; Pan, H.; Wan, D.; Morlet-Savary, F.; Knopf, S. A two-photon active chevron-shaped type I photoinitiator designed for 3D stereolithography. *Chem. Commun.* **2019**, *55*, 6233–6236.
- (9) Hrobarik, P.; Hrobarikova, V.; Sigmundova, I.; Zahradnik, P.; Fakis, M.; Polyzos, I.; Persephonis, P. Benzothiazoles with tunable electron-withdrawing strength and reverse polarity: a route to triphenylamine-based chromophores with enhanced two-photon absorption. *J. Org. Chem.* **2011**, *76*, 8726–8736.
- (10) (a) Hrobarik, P.; Hrobarikova, V.; Semak, V.; Kasak, P.; Rakovsky, E.; Polyzos, I.; Fakis, M.; Persephonis, P. Quadrupolar benzobisthiazole-cored arylamines as highly efficient two-photon absorbing fluorophores. *Org. Lett.* **2014**, *16*, 6358–6361. (b) Hrobarikova, V.; Hrobarik, P.; Gajdos, P.; Fitolis, I.; Fakis, M.; Persephonis, P.; Zahradnik, P. Benzothiazole-based fluorophores of donor- π -acceptor- π -donor type displaying high two-photon absorption. *J. Org. Chem.* **2010**, *75*, 3053–3068. (c) Nociarova, J.; Osusky, P.; Rakovsky, E.; Georgiou, D.; Polyzos, I.; Fakis, M.; Hrobarik, P. Direct Iodination of Electron-Deficient Benzothiazoles: Rapid Access to Two-Photon Absorbing Fluorophores with Quadrupolar D- π -A- π -D Architecture and Tunable Heteroaromatic Core. *Org. Lett.* **2021**, *23*, 3460–3465.
- (11) See, e.g.: (a) Coe, B. J.; Foxon, S. P.; Pilkington, R. A.; Sanchez, S.; Whittaker, D.; Clays, K.; Depotter, G.; Brunschwig, B. S. Nonlinear optical chromophores with two ferrocenyl, octamethylferrocenyl, or 4-(diphenylamino) phenyl groups attached to rhenium(I) or zinc(II) centers. *Organometallics* **2015**, *34*, 1701–1715. (b) Coe, B. J.; Fielden, J.; Foxon, S. P.; Helliwell, M.; Brunschwig, B. S.; Asselberghs, I.; Clays, K.; Olesiak, J.; Matczyszyn, K.; Samoc, M. Quadratic and cubic nonlinear optical properties of salts of diquat-based chromophores with diphenylamino substituents. *J. Phys. Chem. A* **2010**, *114*, 12028–12041. (c) Coe, B. J.; Harris, J. A.; Hall, J. J.; Brunschwig, B. S.; Hung, S. T.; Libaers, W.; Clays, K.; Coles, S. J.; Horton, P. N.; Light, M. E.; Hursthouse, M. B.; Garin, J.; Orduna, J. Syntheses and quadratic nonlinear optical properties of salts containing benzothiazolium electron-acceptor groups. *Chem. Mater.* **2006**, *18*, 5907–5918. (d) Hrobarik, P.; Sigmundova, I.; Zahradnik, P.; Kasak, P.; Arion, V.; Franz, E.; Clays, K. Molecular Engineering of Benzothiazolium Salts with Large Quadratic Hyperpolarizabilities: Can Auxiliary Electron-Withdrawing Groups Enhance Nonlinear Optical Responses? *J. Phys. Chem. C* **2010**, *114*, 22289–22302.
- (12) Zareba, J. K.; Nyk, M.; Samoc, M. Nonlinear Optical Pigments. Two-Photon Absorption in Crosslinked Conjugated Polymers and Prospects for Remote Nonlinear Optical Thermometry. *Polymers* **2020**, *12*, 1670.
- (13) Jin, F.; Rong, Z.; Guo, X.; Ma, M.; Lv, J.; Zhang, L.; Liao, R.; Liu, Y.; Tao, D.; Tian, Y. Novel D- π -A- π -D structural 2, 2'-bipyridine derivatives with different electron donors: Structure, one- and two-photon excited fluorescence and bioimaging. *Dyes Pigm.* **2018**, *150*, 174–180.
- (14) See, e.g.: (a) Lartia, R.; Allain, C.; Bordeau, G.; Schmidt, F.; Fiorini-Debuisschert, C.; Charra, F.; Teulade-Fichou, M. P. Synthetic strategies to derivatizable triphenylamines displaying high two-photon absorption. *J. Org. Chem.* **2008**, *73*, 1732–1744. (b) Belfield, K. D.; Morales, A. R.; Kang, B. S.; Hales, J. M.; Hagan, D. J.; Van Stryland, E. W.; Chapela, V. M.; Percino, J. Synthesis, characterization, and optical properties of new two-photon-absorbing fluorene derivatives. *Chem. Mater.* **2004**, *16*, 4634–4641. (c) Xu, L.; Zhu, H.; Long, G.; Zhao, J.; Li, D.; Ganguly, R.; Li, Y.; Xu, Q.-H.; Zhang, Q. 4-Diphenylamino-phenyl

substituted pyrazine: nonlinear optical switching by protonation. *J. Mater. Chem. C* **2015**, *3*, 9191–9196.

(15) See, e.g.: (a) Beerepoot, M. T.; Friese, D. H.; List, N. H.; Kongsted, J.; Ruud, K. Benchmarking two-photon absorption cross sections: performance of CC2 and CAM-B3LYP. *Phys. Chem. Chem. Phys.* **2015**, *17*, 19306–19314. (b) Rudberg, E.; Salek, P.; Helgaker, T.; Agren, H. Calculations of two-photon charge-transfer excitations using Coulomb-attenuated density-functional theory. *J. Chem. Phys.* **2005**, *123*, 184108.

(16) (a) Ertl, C. D.; Momblona, C.; Pertegás, A.; Junquera-Hernández, J. M.; La-Placa, M.-G.; Prescimone, A.; Ortí, E.; Housecroft, C. E.; Constable, E. C.; Bolink, H. J. Highly Stable Red-Light-Emitting Electrochemical Cells. *J. Am. Chem. Soc.* **2017**, *139*, 3237–3248. (b) Chen, G.-Y.; Chang, B.-R.; Shih, T.-A.; Lin, C.-H.; Lo, C.-L.; Chen, Y.-Y.; Liu, Y.-X.; Li, Y.-R.; Guo, J.-T.; Lu, C.-W.; Yang, Z.-P.; Su, H.-C. Cationic Ir^{III} Emitters with Near-Infrared Emission Beyond 800 nm and Their Use in Light-Emitting Electrochemical Cells. *Chem. - Eur. J.* **2019**, *25*, 5489–5497.

(17) Tian, Z.-Y.; Ming, X.-X.; Teng, H.-B.; Hu, Y.-T.; Zhang, C.-P. Transition-Metal-Free N-Arylation of Amines by Triarylsulfonium Triflates. *Chem. - Eur. J.* **2018**, *24*, 13744–13748.

(18) Sharma, D. K.; Adams, S. T.; Liebmann, K. L.; Miller, S. C. Rapid access to a broad range of 6'-substituted firefly luciferin analogues reveals surprising emitters and inhibitors. *Org. Lett.* **2017**, *19*, 5836–5839.

(19) See, e.g.: (a) Qin, X.; Feng, B.; Dong, J.; Li, X.; Xue, Y.; Lan, J.; You, J. Copper(II)-catalyzed dehydrogenative cross-coupling between two azoles. *J. Org. Chem.* **2012**, *77*, 7677–7683. (b) Li, Y.; Jin, J.; Qian, W.; Bao, W. An efficient and convenient Cu(OAc)₂/air mediated oxidative coupling of azoles via C–H activation. *Org. Biomol. Chem.* **2010**, *8*, 326–330. (c) Fan, S.; Chen, Z.; Zhang, X. Copper-Catalyzed Dehydrogenative Cross-Coupling of Benzothiazoles with Thiazoles and Polyfluoroarene. *Org. Lett.* **2012**, *14*, 4950–4953.

(20) Yang, Y.; Lan, J.; You, J. Oxidative C–H/C–H coupling reactions between two (hetero)arenes. *Chem. Rev.* **2017**, *117*, 8787–8863.

(21) Makarov, N. S.; Drobizhev, M.; Rebane, A. Two-photon absorption standards in the 550–1600 nm excitation wavelength range. *Opt. Express* **2008**, *16*, 4029–4047.

(22) In the three-state model, $\delta_{\text{TPA}}(S_0 \rightarrow S_2)$ of quadrupolar dyes is proportional to $|\mu_{01}|^2|\mu_{12}|^2/(E_1 - E_2/2)^2$ (see Table S10 in SI).

(23) Hrobarik, P.; Hrobarikova, V.; Meier, F.; Repisky, M.; Komarovskiy, S.; Kaupp, M. Relativistic Four-Component DFT Calculations of ¹H NMR Chemical Shifts in Transition-Metal Hydride Complexes: Unusual High-Field Shifts Beyond the Buckingham-Stephens Model. *J. Phys. Chem. A* **2011**, *115*, 5654–5659.